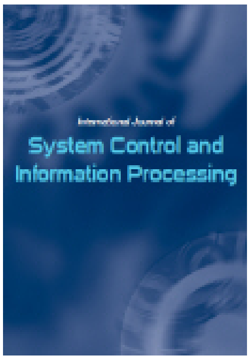

International Journal of System Control and Information Processing

ISSN online: 1759-9342 - ISSN print: 1759-9334
https://www.inderscience.com/ijscip

An ASMDO-based finite time safe control approach for unmanned aerial manipulator

Yanjie Chen, Guohang Zeng, Mengzhao Shen, Xincheng Liu

DOI: 10.1504/IJSCIP.2024.10067150

Article History:

Received:	11 October 2023
Last revised:	15 October 2023
Accepted:	05 August 2024
Published online:	27 June 2025

An ASMDO-based finite time safe control approach for unmanned aerial manipulator

Yanjie Chen*, Guohang Zeng,
Mengzhao Shen and Xincheng Liu

School of Mechanical Engineering and Automation,
Fuzhou University,
Fuzhou, 350108, China
Email: chenyanjiehnu@gmail.com
Email: 220220028@fzu.edu.cn
Email: 220220042@fzu.edu.cn
Email: 220227111@fzu.edu.cn
*Corresponding author

Abstract: Owing to the presence of disturbance and model uncertainties, unmanned aerial manipulator (UAM) may fail to maintain favourable tracking performance while conducting trajectory tracking tasks. To address this problem, this paper presents a safe control approach for UAM to achieve both finite-time convergence of tracking errors and adherence to predefined state constraints. Firstly, an adaptive dual-layer nested structure is applied to construct a disturbance suppressor, guaranteeing the suppression margin converges to a stable range. Then, by designing a nonsingular fast terminal sliding surface for tracking errors and introducing an asymmetric barrier Lyapunov function (BLF), a finite-time safe controller is proposed to achieve finite-time convergence of tracking errors, while guaranteeing the positions remain within the safety constraints. Theoretical analysis is provided to shed light on the properties of both the disturbance suppressor and the finite-time safe controller. Moreover, the effectiveness and feasibility of the proposed control approach are verified through a series of simulation results.

Keywords: UAM; unmanned aerial manipulator; BLF; barrier Lyapunov function; safe control; finite-time control.

Reference to this paper should be made as follows: Chen, Y., Zeng, G., Shen, M. and Liu, X. (2025) 'An ASMDO-based finite time safe control approach for unmanned aerial manipulator', *Int. J. System Control and Information Processing*, Vol. 4, No. 3, pp.235–252.

Biographical notes: Yanjie Chen is with the School of Mechanical Engineering and Automation, Fuzhou University, Fuzhou, China, and with the Key Laboratory of System Control and Information Processing, Ministry of Education, Shanghai, China.

Guohang Zeng received his BS in Mechanical Design Manufacture and Automation in 2022 from Fujian Agricultural and Forestry University, Fuzhou, China, where he is currently working toward the MS in Mechanical Engineering from Fuzhou University, Fuzhou, China. His research interests include unmanned aerial manipulator and visual servoing.

Mengzhao Shen received his BS in Mechatronic Engineering from Anhui Science and Technology University, Chuzhou, China, in 2022, where he is currently working toward the MS in Mechatronic Engineering from Fuzhou University, Fuzhou, China. His research interests include unmanned aerial robot and variable impedance control.

Xincheng Liu received his BS in Mechanical Design Manufacture and Automation in 2022 from Fujian Agricultural and Forestry University, Fuzhou, China, where he is currently working toward the MS in Mechanical Engineering from Fuzhou University, Fuzhou, China. His research interests include aerial interaction and adaptive control.

1 Introduction

As a novel kind of aerial system, an unmanned aerial manipulator (UAM) typically comprises an unmanned aerial vehicle (UAV) and an onboard manipulator. Thanks to high manoeuvrability and versatility, the UAM has been utilised in various tasks in recent years, including fire rescue, environmental monitoring, and cargo transportation (Zhong et al., 2020; Chermprayong et al., 2019). Generally, safety challenges from disturbances in environments and model uncertainties have to be taken into consideration during the daily work of UAM. These factors usually affect the tracking performance of the UAM continuously and may lead to motion instability and even deviations from the desired trajectory. Consequently, the safety issues arising from poor tracking performance and unfavourable errors in trajectory tracking necessitate attention.

To address the issue of safe performance of the UAM, it is advisable to impose safety constraints on the outputs of the UAM system. Safety constraints typically refer to predefined boundaries or limitations, such as positional and attitudinal limitations. As a prevalent method for constraint control, the barrier Lyapunov function (BLF) can guarantee the outputs within the preset range by imposing symmetric constraints on the state variables (Ngo et al., 2005). For example, a nonlinear controller with the BLF was developed to guarantee the quadrotor following a desired trajectory while satisfying the safety constraints imposed on its motion (Kumar et al., 2021). Moreover, a visual servo control method based on a log-type BLF was proposed to impose field of view constraints on the image moment errors to maintain target visibility (Chen et al., 2023). However, practical requirements frequently involve asymmetrical constraints, prompting the development of the asymmetric barrier Lyapunov function (ABLF) for achieving non-symmetric constraints on the outputs. To prevent overshooting of outputs while target tracking, an adaptive neural network controller based on ABLF was proposed to address asymmetric output constraints on a multi-input-multi-output system (He et al., 2017). By integrating a barrier function with the sliding mode control, a finite-time constraint control strategy was developed to achieve stable convergence rates of tracking errors while adhering to the safety constraints (Cruz-Ortiz et al., 2022). Nevertheless, the ABLF method generally assumes prior knowledge of the upper bound of the disturbance, which is difficult to obtain in practical applications. Hence, leveraging the feedback information generated by the sensors becomes imperative to address the dependency issue on the upper-bound functions of disturbances.

The presence of unpredictable external disturbances and model uncertainties affect the dynamic characteristics of UAM, resulting in unsatisfactory control performance and flight stability. Generally, the external disturbance and model uncertainties of the UAM cannot be directly measured. Therefore, treating the uncertainties and external disturbances as an overall disturbance is a common approach to simplify modeling and control (Liang et al., 2022). In order to counteract or compensate for the detrimental impacts, disturbance observer (DOB) has been adopted to enhance the robustness of UAM system. For instance, various DOBs have been developed for disturbance compensation by providing the controller with estimates of disturbances (Zhao et al., 2021; Yang et al., 2013; Xie et al., 2021). However, the DOB encounters the challenge of converging the estimation errors to a bounded range within a finite time, which restricts the applicability of DOB in practical situations requiring rapid dynamic responses. To address the problem, the sliding mode disturbance observer (SMDO) was subsequently developed to drive the estimation error towards a hyperplane within a finite time (Xi et al., 2022; Liu et al., 2022; Edwards and Shtessel, 2016). Without prior knowledge of the upper bounds of disturbances, an adaptive disturbance estimator was designed to achieve the prescribed performance of UAM (Chen et al., 2023). However, although the aforementioned observers can provide valid estimates of disturbances, a globally effective term for disturbance suppression remains unattainable. Therefore, to ensure favourable transient response and stability of UAM, an ASMDO-based disturbance suppressor needs to be designed to accurately estimate disturbances within a finite time, ensuring globally effective suppression of disturbances.

Considering the analysis provided above, a finite-time safe controller based on the adaptive SMDO is proposed to guarantee the convergence of positions of UAM in a finite time while satisfying safety constraints. The main contributions of this paper can be summarised as follows:

- A disturbance suppressor utilising a dual layer adaptive structure of ASMDO is proposed for the UAM system. The external disturbances and model uncertainties can be effectively covered by the disturbance suppressor, and the suppression margins can be driven towards a bounded range within a finite time without prior knowledge of the upper bound of disturbances and their derivatives.
- A finite-time safe controller with a non-singular fast terminal sliding surface is proposed for the UAM system. By presetting the safety boundary, the controller ensures the tracking errors converge to an asymmetric bounded range in a finite time while maintaining positions of UAM within the predetermined safety range.

The rest of this paper is organised as follows: Section 2 introduces the dynamic model of the UAM under external disturbances and model uncertainties. In Section 3, based on the properties of ASMDO, a disturbance suppressor is introduced. Next, a finite-time safe controller for the UAM under asymmetric constraints is presented in Section 4. Subsequently, simulation results are provided in Section 5 to demonstrate the effectiveness of the proposed approach. Finally, some conclusions are presented in Section 6.

2 Dynamics of UAM system

In this section, the dynamics of the UAV and the onboard manipulator under the external disturbance are initially introduced. Then, the dynamics of the UAM are presented by combining the aforementioned dynamics.

Generally, the dynamics of the UAV under external disturbance can be represented as:

$$\begin{cases} \dot{p}_b = v_b \\ m_u \dot{v}_b = f R_b e_3 - m_u g e_3 + F_d \\ \dot{\Phi} = T\omega_b \\ J\dot{\omega}_b = M - \omega_b \times (J\omega_b) + M_d \end{cases} \tag{1}$$

where $p_b = [x, y, z]^\top$ and $\Phi = [\phi, \theta, \psi]^\top$ denote the positions and the Euler angles of the UAV, respectively. $m_u \in R$ denotes the mass, and R_b denotes the rotation matrix, which can be calculated by the Euler angles. Linear velocity and angular velocity of the UAV in the body-fixed frame are defined as $v_b \in R^3$ and $w_b \in R^3$, respectively. g is the acceleration of gravity and $e_3 = [0, 0, 1]^\top$. T denotes the transformation matrix connects the Euler angle rate $\dot{\Phi}$ and the angular velocity ω_b. $J \in R^{3\times3}$ represents the constant inertia matrix. $f = \sum_{i=1}^{4} f_i$ and $M = [M_x, M_y, M_z]^\top$ are the thrust and torque generated by the propellers of UAV, respectively. Generated from the coupling effect of the onboard manipulator and the external disturbances, $F_d \in R^3$ and $M_d \in R^3$ are the interaction force and moment, respectively.

For a n_r-joint onboard manipulator, the dynamics can be represented as:

$$M_m \ddot{q} + C_m \dot{q} + G_m = \tau + \tau_d \tag{2}$$

where $M_m \in R^{n_r \times n_r}$, $C_m \in R^{n_r \times n_r}$, and $G_m \in R^{n_r \times n_r}$ are the positive inertia matrix, centrifugal and Coriolis matrix, and gravity matrix of the onboard manipulator, respectively. $\tau = [\tau_1, \tau_2, ..., \tau_{n_r}]^\top$ denotes the control input, and $\tau_d \in R^{n_r \times 1}$ denotes the interaction force. The joint angles of manipulator are defined as $q = [q_1, q_2, ..., q_{n_r}]^\top$.

Then, let $\eta = [p^\top, \Phi^\top, q^\top]^\top$ denotes the generalised coordinate variable of the UAM. The dynamics of the UAM system under external disturbance can be derived by combining equations (1) and (2), as follows (Fanni and Khalifa, 2017):

$$H(\eta)\ddot{\eta} + C(\eta, \dot{\eta})\dot{\eta} + G(\eta) = u + d_{ext} \tag{3}$$

where $H \in R^{n\times n}$, $C \in R^{n\times n}$, and $G \in R^{n\times 1}$ represent the positive definite inertia matrix, centrifugal and Coriolis matrix and gravity term of the UAM, respectively $(n = 6 + n_r)$. The control input and external disturbance of the UAM are defined as $u \in R^{n\times 1}$ and $d_{ext} \in R^{n\times 1}$, respectively. Moreover, the desired roll angle ϕ_d and pitch angle θ_d can be calculated by the control input u (Yang and Lee, 2014), and the relations between f, M,τ and $u(3)$, …, $u(n)$ are described as follows:

$$\begin{bmatrix} f \\ M \\ \tau \end{bmatrix} = \begin{pmatrix} R_b(3,3) & 0 & 0 \\ 0_{3\times3} & T_b^\top R_b & 0_{3\times3} \\ 0_{nr\times nr} & 0_{nr\times nr} & I_{nr\times nr} \end{pmatrix} \begin{bmatrix} u(3) \\ u(4) \\ \vdots \\ u(n) \end{bmatrix} \tag{4}$$

where $0_{i\times i}$ and $I_{i\times i}$ is zero matrix and identity matrix, respectively, both of the order i.

Generally, the presence of model uncertainties between the actual model and the nominal model of the UAM is inevitable, and the uncertainties can be represented as follows:

$$\begin{cases} H(\eta) - \hat{H}(\eta) = \tilde{H}(\eta) \\ C(\eta, \dot{\eta}) - \widehat{C}(\eta, \dot{\eta}) = \tilde{C}(\eta, \dot{\eta}) \\ G(\eta) - \hat{G}(\eta) = \tilde{G}(\eta) \end{cases} \tag{5}$$

where $\hat{H}$, $\hat{C}$, and $\hat{G}$ represent the nominal model terms of H, C, and G, respectively. The model uncertainties are defined as $\tilde{H}$, $\tilde{C}$, $\tilde{G}$. Moreover, $\hat{H}$ is a positive definite matrix, and the matrix $\dot{\hat{H}}$-2$\hat{C}$ is a skew-symmetrix matrix. Positive constants h_0, c_0, and g_0 exist, satisfying (Roy and Baldi, 2020):

$$\hat{H}^{-1}(\eta) \leq h_0; \hat{C}(\eta, \dot{\eta}) \leq c_0 \left\| \eta_0 \right\|; \hat{G}(\eta) \leq g_0 \tag{6}$$

where $\|\eta_0\|$ denotes the 2-norm of η_0.

Then, substituting equation (5) into equation (3) yields:

$$\begin{aligned} \hat{H}(\eta)\ddot{\eta} + \hat{C}(\eta, \dot{\eta}) + \hat{G}(\eta) &= u + d_{ext} - \tilde{H}(\eta)\ddot{\eta} - \tilde{C}(\eta, \dot{\eta})\dot{\eta} - \tilde{G}(\eta) \\ &= u + d_{ext} - d_{mdl} \\ &= u + d_{ext} - d_{mdl} \\ &= u + a \end{aligned} \tag{7}$$

where d_{ext} and d_{mdl} denote the external disturbance and equivalent disturbance arising from model uncertainties, respectively. Then, the overall disturbance acting on the UAM is denoted as a.

Assumption 1 (Yang et al., 2013)**:** *Assuming that the overall disturbance and its derivative acting on the UAM system during trajectory tracking are bounded, i.e.,* $\|a\| \leq a_0$ *and* $\|\dot{a}\| \leq a_1$*, where* a_0 *and* a_1 *are both unknown constants.*

Considering that the disturbance and its derivatives are typically bounded in practical applications of UAM, the above assumption can be regarded as reasonable.

3 ASMDO-based disturbance suppressor

In this section, by utilising the dual-layer adaptive nested structure of the ASMDO and the properties of the forward invariance set, a globally effective disturbance suppressor is obtained, guaranteeing robustness and stability of UAM during trajectory tracking. Furthermore, the structure of the proposed finite-time safe control approach is shown in Figure 1.

Figure 1 Structure of the proposed finite-time safe control strategy for the UAM system (see online version for colours)

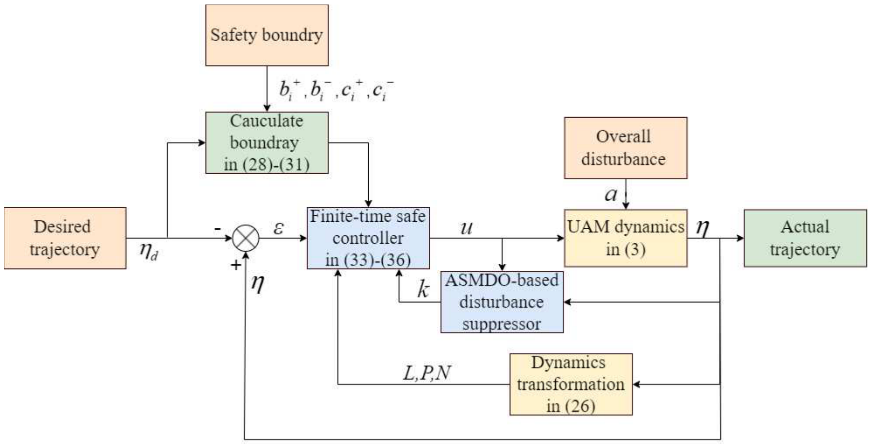

3.1 Design of ASMDO

The primary objective of the section is to derive a disturbance suppression term. Since the disturbance $a(t)$ can only be obtained from the second-order UAM system dynamics, a sliding mode variable $\sigma = \dot{\eta} - \xi$ is introduced to transform the system dynamics into a first-order equation. Based on the UAM dynamics in equation (7), the auxiliary variable ξ is defined to satisfy the following equation:

$$\hat{H}(\eta)\dot{\xi} + \hat{C}(\eta, \dot{\eta})\dot{\eta} + \hat{G}(\eta) = u + z_0\sigma + \nu_1 + \hat{a} \tag{8}$$

where $z_0 = c_0 \|\dot{\eta}\|$, denotes the gain of the sliding surface. $\nu_1 = z_1 \mathrm{sgn}(\sigma)$ and $z_1 = k(t) + \|\hat{a}\| + \overline{\delta}$. The estimated value of a is denoted as $\hat{a}$, and $\overline{\delta}$ is a positive constant. $k(t)$ is introduced to suppress the overall disturbance $a(t)$.

By subtracting equation (8) from equation (7), the following equation can be obtained:

$$\hat{H}\dot{\sigma} = \tilde{a} - z_0\sigma - z_1 \mathrm{sgn}(\sigma) \tag{9}$$

where $\tilde{a}$ denotes the estimation error of disturbance a. The first-order equation can be understood as the convergence rate of the sliding mode variable σ, and the relationship between $\tilde{a}$ and $k(t)$ can be established as σ and $\dot{\sigma}$ tend towards zero. The design of $\overline{\delta}$ and $\mathrm{sgn}(\sigma)$ is aimed at facilitating the proof in Section 3.2, ensuring $k(t)$ remains greater than a.

The ASMDO for UAM is designed as follows:

$$\begin{cases} \hat{a} = \beta + z_2\hat{H}\dot{\eta} \\ \dot{\beta} = z_2(\hat{C}\dot{\eta} + \hat{G} - \dot{\hat{H}}\dot{\eta} - u - \hat{a}) + \nu_2 \\ \nu_2 = (\hat{a}_1 + z_3)\mathrm{sgn}(\nu_1) \\ \dot{\hat{a}}_1 = -c\hat{a}_1 + \|\nu_1\| \end{cases} \tag{10}$$

where c, z_2, and z_3 are positive constants. $\hat{a}_1$ denotes the estimated value of a_1. The $\hat{a}$ serves as an approximation of the disturbance a and is updated based on real-time system feedback.

The nested adaptive structure of ASMDO is designed as:

$$\dot{k}(t) = -\rho(t)\mathrm{sgn}(\delta(t)) \tag{11}$$

$$\dot{r}(t) = \begin{cases} \gamma\,|\delta(t)| & |\delta(t)| > \delta_0 \\ 0 & else \end{cases} \tag{12}$$

$$\dot{\overline{u}}_{eq}(t) = \frac{1}{\tau_s}(-\nu_1 - \overline{u}_{eq}(t)) \tag{13}$$

where $\rho(t) = r_0 + r(t)$ affects the change rate of $k(t)$. r_0 and γ are positive constants. τ_s denotes the sampling time. $\overline{u}_{eq}(t)$ represent an equivalent control, which is formally obtained as the solution $\dot{\sigma} = 0$ when $\sigma = 0$ and satisfies $\overline{u}_{eq}(t) = -a(t)$ (Edwards and Shtessel, 2016).

Then, $\delta(t)$ and $e(t)$ are introduced as follows:

$$\delta(t) = k(t) - \frac{1}{\alpha}|\bar{u}_{\,eq}(t)| - \varepsilon \tag{14}$$

$$e(t) = \frac{qa_1}{\alpha} - r(t) \tag{15}$$

where $\delta(t)$ is employed to demonstrate $k(t) > |a(t)|$ in the subsequent analysis. The parameters ε and α are positive constants affecting the suppression margins between $k(t)$ and absolute values of overall disturbance $|a(t)|$. In addition, α and q are recommended to select in the range $0 < \alpha < 1$ and $q > 1$, respectively.

3.2 *Design of disturbance suppressor*

During the reaching phase of the sliding variables σ, note that $|\mathrm{sgn}(\sigma)| = 1$ holds almost everywhere. According to (13), the equivalent input $|\overline{u}_{eq}(t)| = k(t) + \|\hat{a}\| + \overline{\delta}$ can be derived. Then, $\mathrm{sgn}(\delta(t)) = -1$ can be obtained based on equation (14). Utilising the adaptive law of $k(t)$ from equation (11), $\dot{k}(t) = \rho(t) > r_0$ can be obtained since the derivative of $r(t)$ remains non-negative.

Theorem 1: *Considering the UAM dynamics given by equation (9), the ASMDO designed according to equations (10)–(13) ensures the sliding mode variable σ converges to zero within a finite time during the reaching phase.*

Proof: Considering the following Lyapunov function:

$$V_0 = \sigma^\top \hat{H}\,\sigma \tag{16}$$

The derivative of V_0 can be derived as:

$$\begin{aligned} \dot{V}_0 &= \sigma^\top \dot{\hat{H}}\sigma + 2\sigma^\top \hat{H}\dot{\sigma} \\ &= 2\sigma^\top \hat{C}\,\sigma + 2\sigma^\top(\tilde{a} - z_0\sigma - z_1\mathrm{sgn}(\sigma)) \\ &\leq -2(z_0 - c_0\,\|\dot{\eta}\|)\|\sigma\|^2 - 2(z_1 - \|\tilde{a}\|)\,\|\sigma\| \end{aligned} \tag{17}$$

$$\leq -2(k(t) + \|\hat{a}\| + \overline{\delta} - \|\hat{a}\| - \|a\|)\,\|\sigma\| \leq -2\overline{\delta}\,\|\sigma\|$$
$$\leq \frac{-2\overline{\delta}\sqrt{\sigma^T \hat{H}\,\sigma}}{\sqrt{\lambda_{\max}(\hat{H}\,)}} = \frac{-2\overline{\delta}\sqrt{V}}{\sqrt{\lambda_{\max}(\hat{H}\,)}}$$

Therefore, the sliding mode variable σ converges to zero in a finite time $T_0 = \frac{1}{\frac{2\overline{\delta}}{\sqrt{\lambda_{\max}(\hat{H})}}(1-\frac{1}{2})} = \frac{\lambda_{\max}(\hat{H})}{\overline{\delta}}\sqrt{V(0)}$, where $\lambda_{\max}(A)$ denotes the maximum eigenvalue of matrix A (Bhat and Bernstein, 2000).

During the sliding phase of the sliding variables σ, the parameters are selected to guarantee the boundedness of $\delta(t)$ as follows:

$$\begin{cases} \frac{1}{4}\varepsilon^2 > {\delta_0}^2 + \frac{1}{\gamma}(\frac{qa_1}{\alpha})^2 \\ \frac{1}{\alpha}\,\|\overline{u}_{eq}(t)\| + \frac{\varepsilon}{2} > \|\overline{u}_{eq}(t)\| \\ \left|\frac{\mathrm{d}}{\mathrm{dt}}\overline{u}_{eq}(t)\right| < qa_1 \end{cases} \tag{18}$$

where δ_0 is a small positive constant, and the parameter γ is recommended to be given as a large value to satisfy the first inequality in equation (18).

Assumption 2: *Assuming that the initial value of the overall disturbance $a(t)$ satisfies $a(0) \leq m$, where m is an unknown positive constant.*

To guarantee the inequality $k(t) > |a(t)|$ holds during the reaching phase, a large initial value $k(0)$ and a small positive constant r_0 are recommended to be chosen.

Theorem 2: *Regarding the UAM dynamics in equation (9), the auxiliary variable $\delta(t)$ introduced in equation (14) enters a forward invariant set within a finite time during the sliding phase, under the design of ASMDO according to equations (10)–(13) that satisfies equation (18). Thus, guaranteeing the global effectiveness of the disturbance suppression term $k(t)$.*

Proof: Considering the following Lyapunov function:

$$V_1 = \frac{1}{2}\delta^2 + \frac{1}{2\gamma}e^2 \tag{19}$$

Taking the derivative of V_1 with respect to time:

$$\dot{V}_1 = \delta\dot{\delta} + \frac{1}{\gamma}e\dot{e} \tag{20}$$

Based on equation (14), the time derivative of δ can be given as:

$$\begin{aligned}\dot{\delta}(t) &= \dot{k}(t) - \frac{1}{\alpha}|\dot{u}_{eq}(t)| \\ &= -(r_0 + r(t))\mathrm{sgn}(\delta(t)) - \frac{1}{\alpha}|\dot{u}_{eq}(t)| \\ &= -(r_0 + \frac{qa_1}{\alpha} - e(t))\mathrm{sgn}(\delta(t)) - \frac{1}{\alpha}|\dot{u}_{eq}(t)|\end{aligned}$$

Therefore, the first term of equation (20) can be rewritten as:

$$
\begin{aligned}
\delta(t)\dot{\delta}(t) &= -r_0|\delta(t)| + (e(t) - \frac{qa_1}{\alpha})|\delta(t)| - \frac{1}{\alpha}|\dot{u}_{eq}(t)|\delta(t) \\
&\leq -r_0|\delta(t)| + (e(t) - \frac{qa_1}{\alpha})|\delta(t)| + \frac{qa_1}{\alpha}|\delta(t)| \\
&= -r_0|\delta(t)| + e(t)|\delta(t)|
\end{aligned}
$$

Then, Theorem 2 can be proved under three different conditions A, B, and C, respectively:

Condition A: $|\delta(t)| > \delta_0$

Since the derivative of $e(t)$ can be derived from equation (15), equation (20) becomes:

$$
\begin{aligned}
\dot{V}_0 &= \delta\dot{\delta} + \frac{1}{\gamma}e\dot{e} \\
&\leq -r_0|\delta(t)| + e(t)|\delta(t)| - e(t)|\delta(t)| \\
&\leq -r_0|\delta(t)|
\end{aligned}
$$

According to Barbalat's lemma, $\delta(t) \to 0$ can be derived as $t \to \infty$. Consequently, $\delta(t)$ can be driven to a range of $|\delta(t)| < \frac{\varepsilon}{2}$ within a finite time $T_0 + T_1$.

Based on equation (14), the following inequality can be derived:

$$
\delta(t) = k(t) - \frac{1}{\alpha}|\overline{u}_{eq}(t)| - \varepsilon > -\frac{\varepsilon}{2} \tag{21}
$$

Consequently, the disturbance suppression term $k(t)$ can be expressed as:

$$
k(t) > \frac{\varepsilon}{2} + \frac{1}{\alpha}|\overline{u}_{eq}(t)| > |\overline{u}_{eq}(t)| = |a(t)| \tag{22}
$$

Condition B: $|\delta(t)| \leq \delta_0$, $e(t) \leq 0$

In this condition, the inequalities $\dot{V}_0 \leq -r_0|\delta(t)|$ and $k(t) > |a(t)|$ can be similarly derived.

Condition C: $|\delta(t)| \leq \delta_0$ and $e(t) > 0$

The initial value of $r(t)$ is designed as a positive constant. Thereafter, $r(t) \geq 0, \forall t > 0$ can be obtained based on equation (12).

According to the definition of $e(t)$ in equation (15), $e(t) \leq \frac{qa_1}{\alpha}$ can be derived. Then, a rectangle domain Γ is defined for subsequent theoretical analysis as follows:

$$
\Gamma = \left\{(\delta, e) : |\delta| < \delta_0, 0 \leq e < \frac{qa_1}{\alpha}\right\} \tag{23}
$$

Notice that the inequality $\dot{V}_0 \leq -r_0|\delta(t)|$ holds when the combination (δ, e) falls outside of Γ, and an ellipse domain centered at the origin is introduced as

$$
\overline{\Gamma} = \{(\delta, e) : V_1(\delta, e) < \overline{r}\} \tag{24}
$$

where $\overline{r} = \frac{1}{2}{\delta_0}^2 + \frac{1}{2\gamma}(\frac{qa_1}{\alpha})^2$ is a positive constant.

Based on the properties of ellipses, the vertex of the rectangular domain Γ is located on the ellipse. As a result, $\Gamma \subset \overline{\Gamma}$, as shown in Figure 2.

Note that the domain outside of $\overline{\Gamma}$ satisfies $\dot{V}_0 \leq -r_0|\delta(t)|$ and therefore, $\overline{\Gamma}$ can be regarded as a forward invariant set. Then, the inequality $|\delta(t)| < \frac{\varepsilon}{2}$ can be obtained in a finite time according to Barbalat's Lemma, and $k(t) > |a(t)|$ holds based on the analysis given in condition A.

Figure 2 the domain of Γ and $\overline{\Gamma}$ (see online version for colours)

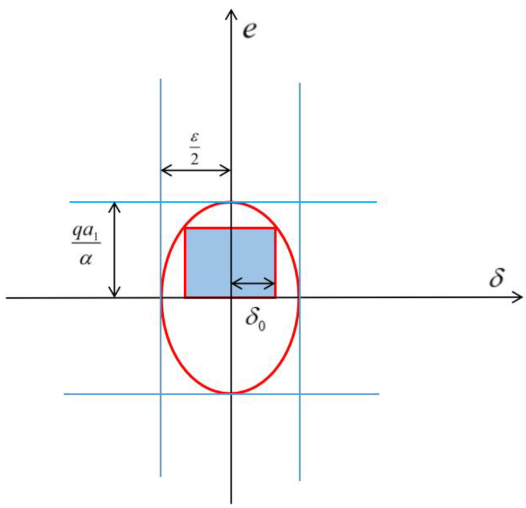

To summarise, guaranteeing a large value of $k(0)$ and small value of r_0 can prevent $\delta(t)$ from entering the range $(-\infty, -\delta_0)$ during the reaching phase. Consequently, only two situations remain for $\delta(T_0)$:

Situation 1: $\delta(T_0) \in (-\delta_0, \delta_0)$, and the inequality $k(t) > |a(t)|$ can be indicated according to condition B and condition C.

Situation 2: $\delta(T_0) \in (\delta_0, +\infty)$, and the combination (δ, e) falls outside the domain $\overline{\Gamma}$. Therefore, the inequality $|\delta(t)| < \frac{\varepsilon}{2}$ can be guaranteed in a finite time $T_0 + T_1$ thanks to the property of $\dot{V}_0 \leq -r_0|\delta(t)|$. Consequently, given the validity of $\delta(t) = k(t) - \frac{1}{\alpha}|\bar{u}_{eq}(t)| - \varepsilon > \frac{\varepsilon}{2}$, the inequality $k(t) > \frac{3\varepsilon}{2} + \frac{1}{\alpha}|\bar{u}_{eq}(t)| > |\bar{u}_{eq}(t)| = |a(t)|$ can be deduced.

Therefore, $k(t) > |a(t)|$ can be guaranteed during the reaching phase and sliding phase by taking a large initial value of $k(t)$ and a small value of r_0.

4 Design of finite-time safe controller

In this section, based on the properties of the non-singular fast terminal sliding surface and ABLF, a finite-time safe controller is designed to achieve finite-time convergence of the tracking errors under asymmetric constraints on outputs of UAM.

By transforming equation (7) into a second-order equation with respect to η, the dynamics of UAM can be rewritten as

$$\ddot{\eta} = L + Pu + N \tag{25}$$

where $L = -\hat{H}^{-1}\hat{C}\dot{\eta} - \hat{H}^{-1}\hat{G}$, $P = \hat{H}^{-1}$, and $N = \hat{H}^{-1}a$. Let $\hat{H}^{-1}k(t) = \overline{N}(t)$, the inequality $N(t) \leq \overline{N}(t)$ can be obtained since $k(t) > |a(t)|$.

The tracking error of η is defined as $\varepsilon = \eta - \eta_d$, and η_d represents the expected value of the generalised vector η. Based on equation (25), the second derivative of error ε can be derived as:

$$\ddot{\varepsilon} = \ddot{\eta} - \ddot{\eta}_d = L + Pu + N - \ddot{\eta}_d \tag{26}$$

By decoupling (26), the error dynamics of each subsystem can be expressed as

$$\ddot{\varepsilon}_i = l_i(\eta) + p_i(\eta_{1,i})u_i + \sum_{i=1, i\neq j}^{n} p_{i,j}(\eta_1)u_j + n_i(\eta_1, t) - \ddot{\eta}_{d,i} \tag{27}$$

where $\ddot{\varepsilon}_i$, l_i, u_i, and n_i are the ith element of $\ddot{\varepsilon}$, L, u, and N, respectively. The value of p_i is the element located at the ith row and ith column of matrix P, and the matrix $p_{i,j}$ aggregates the influence of the remaining control input u_j when $i \neq j$.

To guarantee the safety performance during trajectory tracking, the generalised coordinate variables η_i and its derivatives are upper and lower bounded by b_i^+, c_i^+, b_i^-, and c_i^-, respectively. Similarly, the upper and lower bounds for η_d and $\dot{\eta}_d$ are set as $y_{1,i}^+$, $y_{1,i}^-$, $y_{2,i}^+$, and $y_{2,i}^-$, respectively. Therefore, the upper and lower bounds for the errors $\underline{\varepsilon}_i$, $\overline{\varepsilon}_i$, $\underline{d\varepsilon}_i$, and $\overline{d\varepsilon}_i$ are defined as:

$$\begin{cases} \underline{\varepsilon}_i = b_i^- - y_{1,i}^+ \\ \overline{\varepsilon}_i = b_i^+ - y_{1,i}^- \\ \underline{d\varepsilon}_i = c_i^- - y_{2,i}^+ \\ \overline{d\varepsilon}_i = c_i^+ - y_{2,i}^- \end{cases} \tag{28}$$

To design the finite-time safe controller, the non-singular fast terminal sliding surface is introduced as follows:

$$s_i = \varepsilon_i + \frac{1}{\kappa_1}\varepsilon_i^{\frac{g}{h}} + \kappa_2 \dot{\varepsilon}_i^{\frac{p}{q}} \tag{29}$$

where g, h, p, and q are all odd numbers. These parameters are selected to satisfy $\frac{g}{h} > \frac{p}{q}$ and $1 < \frac{p}{q} < 2$. The sliding mode gains κ_1 and κ_2 are positive constants, affecting the convergence rate of s_i. Then, the desired lower and upper bounds of the sliding variables s_i are defined as:

$$\underline{s}_i = \underline{\varepsilon}_i + \frac{1}{\kappa_1}\underline{\varepsilon}_i^{\frac{g}{h}} + \kappa_2 \underline{d\varepsilon}_i^{\frac{p}{q}} \tag{30}$$

$$\overline{s}_i = \overline{\varepsilon}_i + \frac{1}{\kappa_1}\overline{\varepsilon}_i^{\frac{g}{h}} + \kappa_2 \overline{d\varepsilon}_i^{\frac{p}{q}} \tag{31}$$

Define the normalised variable $\lambda_{a,i} = \frac{s_i}{\underline{s}_i}$ and $\lambda_{b,i} = \frac{s_i}{\overline{s}_i}$, satisfying that $0 < \lambda_{a,i} \leq 1$ when $s_i < 0$ and $0 < \lambda_{b,i} \leq 1$ when $s_i > 0$, respectively. Subsequently, the unit step function $\Omega(a)$ is introduced as :

$$\Omega(a) = \begin{cases} 1 & a > 0 \\ 0 & a \leq 0 \end{cases} \tag{32}$$

The control law for each subsystem of UAM is defined as:

$$u_i = u_{eq,i} + u_{bs,i} \tag{33}$$

$$u_{eq,i} = p_i^{-1}(-l_i - \sum_{i=1,i\neq j}^{n} p_{i,j}(\eta_1)u_j + \ddot{\eta}_{d,i}) \tag{34}$$

$$u_{bs,i} = \frac{q}{\kappa_2 p}\dot{\varepsilon}_i^{(1-\frac{p}{q})} p_i^{-1}(-\varepsilon_i - \kappa_1 \frac{g}{h}\varepsilon_i^{(\frac{g}{h}-1)}\dot{\varepsilon}_i) - \varpi_i \mathrm{sgn}(s_i) \tag{35}$$

where the term $u_{eq,i}$ is utilised to offset the known components in the subsystem, and the term $u_{bs,i}$ is designed to compensate for the uncertainties and drive the sliding variable s_i converging to zero. Then, the control gains in equation (35) are given as follows:

$$\varpi_i(t) = \begin{cases} (\frac{1}{2})^{\frac{3}{2}}\overline{s}_i\mu_i\frac{1}{1-\lambda_{b,i}} + \kappa_2\frac{p}{q}\dot{\varepsilon}^{(\frac{p}{q}-1)}\mathrm{sgn}(\eta_{b,i})\frac{\overline{N}_i}{1-\lambda_{b,i}} & s_i > 0 \\ -(\frac{1}{2})^{\frac{3}{2}}\underline{s}_i\mu_i\frac{1}{1-\lambda_{a,i}} - \kappa_2\frac{p}{q}\dot{\varepsilon}^{(\frac{p}{q}-1)}\mathrm{sgn}(\eta_{a,i})\frac{\overline{N}_i}{1-\lambda_{a,i}} & s_i < 0 \end{cases} \tag{36}$$

where $\overline{N}_i$ denotes the i-th component of $\overline{N}$.

Theorem 3: *For the UAM system in equation (25), if the sliding mode variable s and controller are designed as (29) and (33), the tracking error ε can be driven to zero within a finite time.*

Proof: Consider the asymmetric barrier Lyapunov function of ith subsystem:

$$\begin{aligned} V_i &= \frac{\Omega(s_i)}{2}\log(\frac{\overline{s}_i^2}{\overline{s}_i^2 - s_i^2}) + \frac{1-\Omega(s_i)}{2}\log(\frac{\underline{s}_i^2}{\underline{s}_i^2 - s_i^2}) \\ &= \frac{1}{2}\log\frac{1}{1-\lambda_i^2} \end{aligned} \tag{37}$$

where $\lambda_i = \Omega\left(s_i\right)\lambda_{b,i} + (1-\Omega\left(s_i\right))\lambda_{a,i}$ represents a binary function with $\lambda_i \in [0,1]$.

Then, according to the definition of s_i in equation (29), the time derivative of s_i can be derived as:

$$\begin{aligned} \dot{s}_i &= \dot{\varepsilon} + \frac{1}{\kappa_1}\gamma_1 \mathrm{sig}^{\gamma_1 - 1}(\varepsilon_\mathrm{i})\dot{\varepsilon}_\mathrm{i} + \kappa_2\gamma_2 \mathrm{sig}^{\gamma_2 - 1}(\dot{\varepsilon}_\mathrm{i})\ddot{\varepsilon}_\mathrm{i} \\ &\leq -\varpi_i(t)\mathrm{sgn}(s_i) + n_i(t) \end{aligned} \tag{38}$$

where $\gamma_1 = \frac{p}{q}$, $\gamma_2 = \frac{g}{h}$ and the function $\mathrm{sig}^a(x)$ denotes $x^a\mathrm{sgn}(x)$.

Let $\zeta_i = \frac{\Omega(s_i)}{\overline{s}_i^2 - s_i^2} + \frac{1-\Omega(s_i)}{\underline{s}_i^2 - s_i^2}$ and combining with equation (38), the $\dot{V}_i$ can be obtained as:

$$\dot{V}_i = \zeta_i s_i \dot{s}_i \leq -\frac{\Omega(s_i)\lambda_{b,i}}{\overline{s}_i(1-\lambda_{b,i}^2)}(\varpi_i(t)\text{sgn}(s_i) + n_i(t)) \\ + \frac{(1-\Omega(s_i))\lambda_{a,i}}{\underline{s}_i(1-\lambda_{a,i}^2)}(\varpi_i(t)\text{sgn}(s_i) + n_i(t)) \tag{39}$$

Substituting the control gains (36) into (39), the time derivative of V_i can be reformulated as:

$$\dot{V}_i \leq -\Omega(s_i)\frac{\lambda_{b,i}^2}{1-\lambda_{b,i}^2}\frac{0.5\cdot\mu_i}{\eta_{b,i}} - (1-\Omega(s_i))\frac{\lambda_{a,i}^2}{1-\lambda_{a,i}^2}\frac{0.5\cdot\mu_i}{\lambda_{a,i}} \\ \leq -\mu_i\sqrt{0.5}(\Omega(s_i)\sqrt{\frac{1}{2}\log(\frac{1}{1-\lambda_{b,i}^2})} + \Omega(s_i)\sqrt{\frac{1}{2}\log(\frac{1}{1-\lambda_{a,i}^2})}) \tag{40}$$

Then, according to the Cauchy-Schwarz inequality $\sqrt{a} + \sqrt{b} \geq \sqrt{a+b}$ and $V(s(t)) = \sum_{i=1}^{n} V_i(s_i(t))$, the derivative of V with respect to time can be derived as:

$$\dot{V} \leq -\sqrt{0.5}\sum_{i=1}^{n}\mu_i\sqrt{V}_i \leq -\sqrt{0.5}\overline{u}\sqrt{V} \tag{41}$$

where $\overline{u}$ = min (u_i), $i = 0, 1, ..., n$. Therefore, the sliding mode variable s_i can converge to zero within a finite time (Bhat and Bernstein, 2000), and the tracking error ε_i can also be driven to zero in a finite time after $s_i = 0$.

5 Simulation results and analysis

In this section, a series of simulation results are presented to illustrate the feasibility and tracking performance of the proposed safe control method. Comparative simulations are conducted among the proposed method, an ABSMC method (Mireles et al., 2022), and a NFTSMC method (Zhu et al., 2021), with an emphasis on highlighting the rapid dynamic performance and constraint satisfaction performance of the proposed method.

5.1 Simulation setup

The simulations were conducted in MATLAB/Simulink to demonstrate the effectiveness of the proposed control method. The utilised UAM model comprises a four-rotor unmanned aerial vehicle and a 2-DOF onboard manipulator. To simulate the external disturbance and model uncertainties of the UAM, the overall disturbance is given as $a_i = A_i\eta_i + B_i \sin t$, where $A_i = [0.5; 0.5; 0.5; 0.2; 0.2; 0.2; 0.1; 0.1]$ and $B_i = [2; 1.5; 1; 0.5; 0.3; 0.2; 0.8; 0.6]$. The desired position trajectory is set as $p_d = [0.5\sin t - 0.2, 0.5\sin t - 0.2, 0.5\sin t - 0.2]^\top$, $\psi_d = 0$ and $q_d = [0.4\sin t, 0.4\sin t]^\top$. The parameters used in the ASMDO-based disturbance suppressor are chosen as: $\alpha = 0.95, \gamma = 10^4, r_0 = 0.5, \overline{\delta} = 0.5, \varepsilon = 0.1, z_2 =$

$20, z_3 = 2, c_0 = 10, c = 0.5, \tau = 0.01$. Safety constraint boundaries for the positions x, y, z are set as: $b_i^+ = 0.4, b_i^- = -0.8, c_i^- = -1.1$, and $c_i^+ = 1.1$, respectively. The parameters of finite-time safe controller are selected as $\kappa_1 = 50, \kappa_2 = 0.5, g = 11, h = 9, p = 7$, and $q = 5$. To validate the effectiveness of the proposed finite-time safe control method, simulations are conducted in MATLAB. The disturbance suppression term $k(t)$ is derived from the proposed disturbance suppressor and then transmitted to the safe finite-time controller, which computes the control signal for the UAM. Subsequently, the feasibility of the proposed method can be verified by comparing the values between $k(t)$ and the preset disturbance $a(t)$, as well as the actual trajectory $p = [x, y, z]^\top$ and the desired trajectory $p_d = [x_d, y_d, z_d]^\top$. Moreover, in order to reduce the chattering caused by the sign function, the boundary layer function is used instead of the sign function, with the boundary taken as $\Delta = 0.05$.

5.2 Simulation results

To validate the correctness of the proposed approach, the UAM pursues the predefined helical trajectory $p_d = [\cos(t), \sin(t), 2t]^\top$. Figure 3 illustrates the trajectory tracking performance of the UAM in three-dimensional space using the proposed controller, and it can be observed from the depicted image that the UAM successfully tracks the expected trajectory.

Figure 3 3D spiral trajectory tracking of the UAM (see online version for colours)

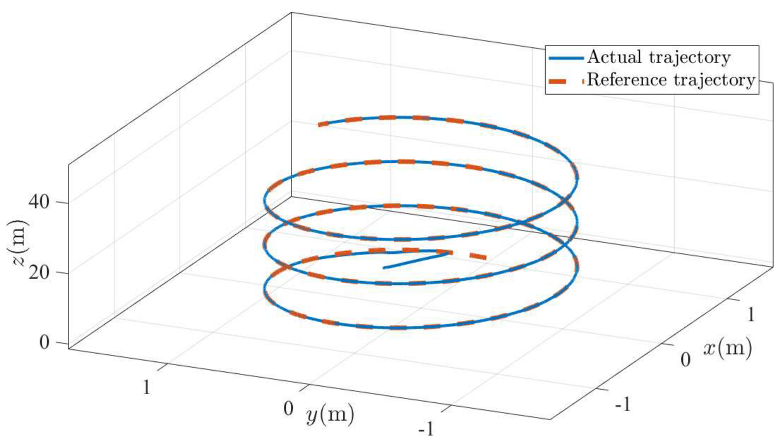

The comparison results are shown in Figures 4 and 5. As shown in Figure 4(a) and (c), it can be observed that the $k(t)$ given by the proposed suppressor is always larger than the absolute value of the disturbance $a(t)$, thereby satisfying the inequality $k(t) > |a(t)|$. In order to guarantee the effectiveness of the disturbance suppressor even before the sliding stage, a large initial value of $k(t)$ is advisable. Then, the suppression margins can converge to a stable range within a finite time owing to the nested adaptive structure of ASMDO, and the margins are influenced by the parameters α and ε. Additionally, the convergence has been demonstrated to exhibit generality by selecting various initial values of k.

Figure 4 Performances of disturbance suppressor: (a) performances on positions of the UAM; (b) performances on attitudes of the UAM and (c) performances on joint-angles of the UAM (see online version for colours)

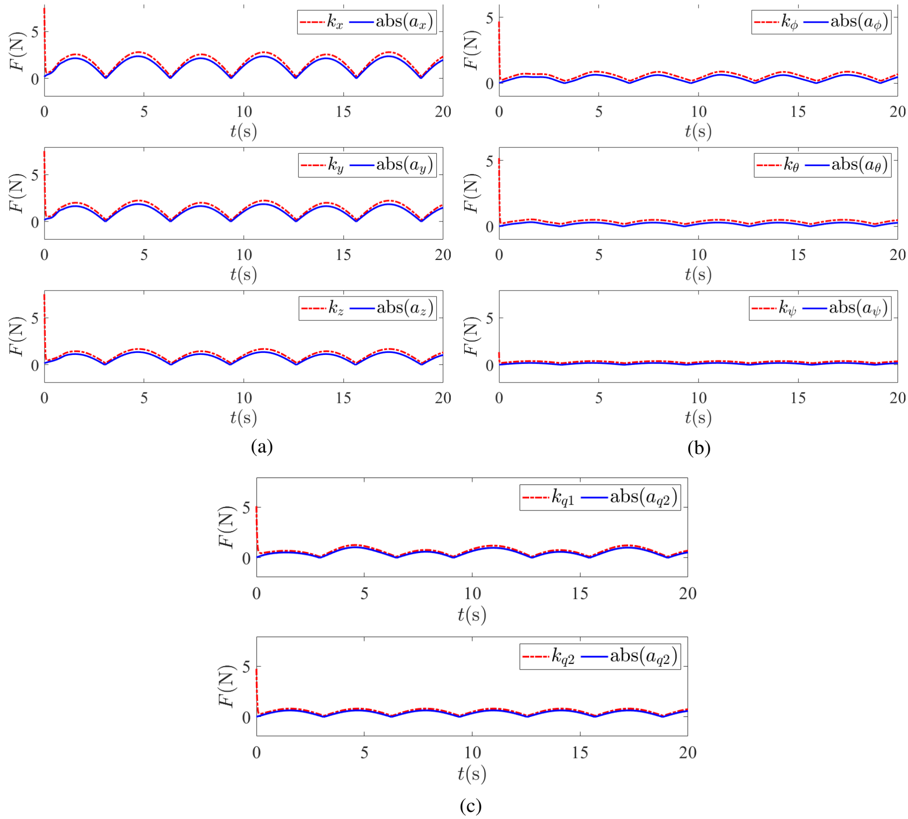

To demonstrate the performance of the proposed finite-time safe controller, comparative simulations were conducted with the ABSMC (Mireles et al., 2022) and the NFTSMC (Zhu et al., 2021). For the sake of equitable comparisons, the methods mentioned above are subjected to the identical disturbance $a(t)$. The comparison results of position trajectory tracking are depicted in Figure 5. It is observed that the proposed control approach can rapidly and accurately follow the desired curve, exhibiting faster convergence rates and smaller overshoots both in the x-, y-, and z-direction. Despite the NFTSMC method exhibits performance in achieving finite time convergence of tracking errors, the NFTSMC method lacks the capability to guarantee the positions within the desired safety range, thus resulting in positional values of x, y, and z slightly exceeding the safety constraints in the time period $t = 0 \sim 5$ s.

To further validate the robustness of the proposed control method, the steady-state error statistics and convergence time of the simulation results are shown in Table 1. As shown in the table, root mean squared error (RMSE) and standard deviation (STD) represent root mean square error and standard deviation, respectively. Note that the RMSE, STD, and convergence times of the proposed method are lower than those in the ABSMC method, indicating that the proposed strategy demonstrates enhanced robustness and dynamic response performance while maintaining safety constraints.

Figure 5 Position trajectory tracking of the UAM (see online version for colours)

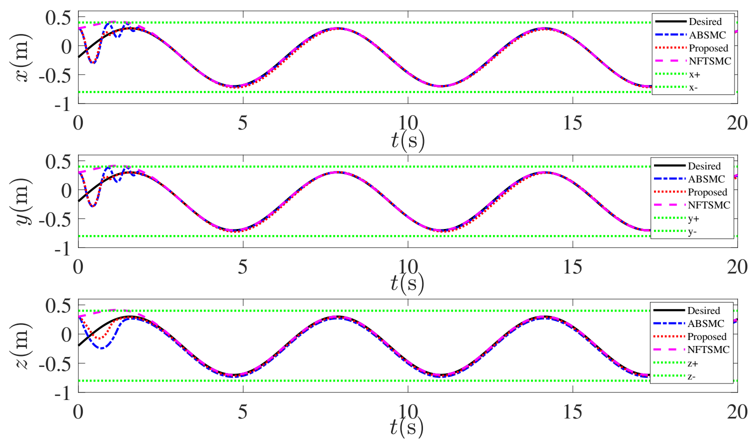

Table 1 Steady-state error statistics of the proposed method and comparison method in the simulations

	Proposed method			*ABSMC*		
	RMSE	*STD*	t(s)	*RMSE*	*STD*	t(s)
x(m)	0.0442	0.0438	0.819	0.0577	0.0571	1.538
y(m)	0.0443	0.0438	0.977	0.0567	0.0559	1.546
z(m)	0.0563	0.0559	1.099	0.1307	0.1256	1.595

6 Conclusion

In this paper, a finite-time safe control approach has been proposed to address trajectory tracking of UAM with state constraints. The dynamics of UAM were given, with the external disturbance and model uncertainties regarded as the overall disturbance. To cover the adverse influence brought by the disturbance, an ASMDO-based suppressor was proposed without prior knowledge of the overall disturbance and its derivatives. Subsequently, to enable fast and stable convergence of the tracking errors while adhering to the safety constraints, a finite-time safe controller was proposed by employing the properties of non-singular fast terminal sliding mode surface and ABLF. Theoretical analysis and Lyapunov stability proofs were provided for the proposed disturbance suppressor and the finite-time safe controller. Then, the feasibility and stability of the proposed control method were verified through simulations.

Acknowledgements

This work was supported in part by the National Natural Science Foundation of China (No. 62273098) and the Foundation of Key Laboratory of System Control and Information Processing, Ministry of Education, China (No. Scip202201).

References

Bhat, S.P. and Bernstein, D.S. (2000) 'Finite-time stability of continuous autonomous systems', *Siam J. Contr. Opti*, Vol. 38, No. 3, pp.751-766.

Chaikalis, D., Khorrami, F. and Tzes, A. (2020) 'Adaptive control approaches for an unmanned aerial manipulation system', *2020 International Conference on Unmanned Aircraft Systems (ICUAS)*, Athens, Greece, pp.498–503.

Chen, Y., Zhan, W., He, B., Lin, L., Miao, Z., Yuan, X. and Wang, Y. (2020) 'Robust control for unmanned aerial manipulator under disturbances', *IEEE Access*, Vol. 8, pp.129869–129877.

Chen, Y., Wu, Y., Zhang, Z., Miao, Z., Zhong, H., Zhang, H. and Wang, Y. (2023) 'Image-based visual servoing of unmanned aerial manipulators for tracking and grasping a moving target', *IEEE Transactions on Industrial Informatics*, Vol. 19, No. 8, pp.8889–8899.

Chen, Y., Liang, J., Wu, Y., Miao, Z., Zhang, H. and Wang, Y. (2023) 'Adaptive sliding-mode disturbance observer-based finite-time control for unmanned aerial manipulator with prescribed performance', *IEEE Transactions on Cybernetics*, Vol. 53, No. 5, pp.3263–3276.

Chermprayong, P., Zhang, K., Xiao, F., and Kovac, M. (2019) 'An integrated delta manipulator for aerial repair: a new aerial robotic system', *IEEE Robotics and Automation Magazine*, Vol. 26, No. 1, pp.54–66.

Cruz-Ortiz, D., Chairez, I. and Poznyak, A. (2022) 'Sliding-mode control of full-state constraint nonlinear systems: a barrier Lyapunov function approach', *IEEE Transactions on Systems, Man, and Cybernetics: Systems*, Vol. 52, No. 10, pp.6593–6606.

Edwards, C. and Shtessel, Y.B. (2016) 'Adaptive continuous higher order sliding mode control', *Automatica*, Vol. 65, pp.183–190.

Fanni, M. and Khalifa, A. (2017) 'A new 6-DOF quadrotor manipulation system: design, kinematics, dynamics, and control', *IEEE/ASME Transactions on Mechatronics*, Vol. 22, No. 3, pp.1315–1326.

He, W., Yin, Z. and Sun, C. (2017) 'Adaptive neural network control of a marine vessel with constraints using the asymmetric barrier lyapunov function', *IEEE Transactions on Cybernetics*, Vol. 47, No. 7, pp.1641–1651.

Kumar, S. and Kumar, S. R. (2022) 'Barrier lyapunov-based nonlinear trajectory following for unmanned aerial vehicles with constrained motion', *2022 International Conference on Unmanned Aircraft Systems (ICUAS)*, Dubrovnik, Croatia, pp.1146–1155.

Li, B., Wen, S., Yan, Z., Wen, G. and Huang, T. (2023) 'A survey on the control Lyapunov function and control barrier function for nonlinear-affine control systems', *IEEE/CAA Journal of Automatica Sinica*, Vol. 10, No. 3, pp.584–602.

Liang, J., Chen, Y., Lai, N., He, B., Miao, Z. and Wang, Y. (2022) 'Low-complexity prescribed performance control for unmanned aerial manipulator robot system under model uncertainty and unknown disturbances', *IEEE Transactions on Industrial Informatics*, Vol. 18, No. 7, pp.4632–4641.

Liu, W., Chen, M. and Shi, P. (2022) 'Fixed-time disturbance observer-based control for quadcopter suspension transportation system', *IEEE Transactions on Circuits and Systems I: Regular Papers*, Vol. 69, No. 11, pp.4632–4642.

Mireles-Perez, C., Gomez-Correa, M., Curz-Ortiz, D., Ballesteros, M. and Salgado, I. (2022) 'First-order sliding mode control for second order systems with asymmetric constraints', *2022 10th International Conference on Systems and Control (ICSC)*, Marseille, France, pp.227–232.

Ngo, K., Mahony, R. and Jiang, Z. (2005) 'Integrator backstepping using barrier functions for systems with multiple state constraints', *Proceedings of the 44th IEEE Conference on Decision and Control*, Seville, Spain, pp.8306–8312.

Roy, S. and Baldi, S. (2020) 'Towards structure-independent stabilization for uncertain underactuated Euler–Lagrange systems', *Automatica*, Vol. 113, pp.1–8.

Ryll, M., Bülthoff, H. and Giordano, P. (2015) 'A novel overactuated quadrotor unmanned aerial vehicle: modeling, control, and experimental validation', *IEEE Transactions on Control Systems Technology*, Vol. 23, No. 2, pp.540–556.

Shakhatreh, H., Sawalmeh, A.H., Al-Fuqaha, A., Dou, Z., Almaita, E., Khalil, I., Othman, N.S., Khreishah, A. and Guizani, M. (2019) 'Unmanned aerial vehicles (UAVs): a survey on civil applications and key research challenges', *IEEE Access*, Vol. 7, pp.48572–48634.

Xi, R., Xiao, X., Ma, T. and Yang, Z. (2022) 'Adaptive sliding mode disturbance observer based robust control for robot manipulators towards assembly assistance', *IEEE Robotics and Automation Letters*, Vol. 7, No. 3, pp.6139–6146.

Xie, T., Hu, W., Shao, H., Zeng, W. and Li, G. (2021) 'Nonlinear disturbance observer based sliding mode tracking control for robotic manipulators', *2021 IEEE International Conference on Networking, Sensing and Control (ICNSC)*, Xiamen, China, pp.1–5.

Yang, H. and Lee, D. (2014) 'Dynamics and control of quadrotor with robotic manipulator', *2014 IEEE International Conference on Robotics and Automation (ICRA)*, Hong Kong, China, pp.5544–5549.

Yang, J., Li, S. and Yu, X. (2013) 'Sliding-mode control for systems with mismatched uncertainties via a disturbance observer', *IEEE Transactions on Industrial Electronics*, Vol. 60, No. 1, pp.160–169.

Zhang, G., He, Y., Dai, B., Gu, F., Han, J. and Liu, G. (2020) 'Robust control of an aerial manipulator based on a variable inertia parameters model', *IEEE Transactions on Industrial Electronics*, Vol. 67, No. 11, pp.9515–9525.

Zhao, Y., Li, X. and Song, S. (2021) 'Observer-based sliding mode control for stabilization of mismatched disturbance systems with or without time delays', *IEEE Transactions on Systems, Man, and Cybernetics: Systems*, Vol. 51, No 12, pp.7337–7345.

Zhong, H., Miao, Z., Wang, Y., Mao, J., Li, L., Zhang, H., Chen, Y. and Firreo. R. (2020) 'A practical visual servo control for aerial manipulation using a spherical projection model', *IEEE Transactions on Industrial Electronics*, Vol. 67, No. 12, pp.10564–10574.

Zhu, Y., Wu, D. and Li, S. (2021) 'Non-singular fast terminal sliding mode tracking control of a 2-DOF robotic manipulator using finite-time extended State Observer', *2021 33rd Chinese Control and Decision Conference (CCDC)*, Kunming, China, pp.4713–4718.